Proceedings of the ASME International Mechanical Engineering Congress & Exposition
IMECE 2012
November 9-15, 2012, Houston, Texas, USA

IMECE2012-86363

AERODYNAMIC AND ELECTROMAGNETIC ANALYSIS OF A VARIABLE ELECTROMOTIVE-FORCE GENERATOR FOR A WIND TURBINE

N. Goudarzi
Mechanical Engineering Department
University of Maryland, Baltimore County
Baltimore, MD 21250
navid2@umbc.edu

W. D. Zhu
Mechanical Engineering Department
University of Maryland, Baltimore County
Baltimore, MD 21250
wzhu@umbc.edu

R. Bowers
Economics Department
University of Maryland, Baltimore County
Baltimore, MD 21250
bowers1@umbc.edu

ABSTRACT

A question that usually arises is whether an existing wind turbine with a specified rotor can be modified to expand its operational range and improve the power generation. There are various methods to achieve this goal and one of them can be a modified generator referred to as a variable electromotive-force generator (VEG), where the overlap between the rotor and the stator is made to be adjustable. In this work the possibility of harnessing more wind power via a VEG in areas with large changes in the wind speed from very low to high values throughout a year is investigated theoretically. Aerodynamic and mathematical techniques are used to estimate the generated power of a wind turbine in the low wind speed region, and a combination of electromagnetic and aerodynamics principles are employed to obtain the mathematical model of the VEG with an adjustable overlap between the rotor and the stator. The Neg-Micon wind turbine (NM-72) specifications for a certain site in Thailand are used for the numerical analysis. The results show the possibility of expanding the operational range and increasing the power generation of the studied wind turbine.

NOMENCLATURE

A	Rotor Swept Area - m^2
B	Magnetic Flux Density - Wb/m^2
C_P	Power Coefficient
C_{Pmax}	Maximum Power Coefficient
Ds	Change in the Magnetic Field Length - m
E_a	Electromotive Force – V
G	Gravitational Constant - m/s^2
H	Height – m
I_a	Current – Amp
l_f	Width of the Magnetic Field – m
N	Number of Coils
P	True Power of a Synchronous Generator – W
P_0	Sea-Level Atmospheric Pressure – Pa
P_g	Output Generator Power – W
P_{gci}	Output Generator Power at the Cut-in Speed – W
P_{gi}	Output Generator Power at An Arbitrary Input Wind Speed – W
P_r	Output Rotor Power – W
P_{pm}	Output Rotor Power – W
P_{rci}	Output Rotor Power at the Cut-in Speed - Nm/s
P_{ri}	Output Rotor Power at An Arbitrary Input Wind Speed – W

Q	Reactive Power of a Synchronous Generator – VAR
R	Resistance – Ohm
S	Apparent Power of a Synchronous Generator – VA
T	Torque – N.m
T_e	Temperature – K
U	Wind Speed- m/s
V_a	Terminal Voltage – V
X	Reactance – Ohm
Z	Impedance – Ohm
α	Axial Induction Factor
δ	Load Angle
η / η_{mech}	Efficiency/Mechanical Efficiency
θ	Phase Angle
ω	Rotational Speed - rad/s
Φ	Magnetic Flux – Wb
	Air Density - kg/m^3
λ	Tip Speed Ratio

1. INTRODUCTION

Renewable energy technologies, such as wind power, solar power, hydropower, and biomass, can reduce the emission of greenhouse gases significantly and at a same time reduce the dependency on the oil industry. Within these resources, one of the most important and developed is the wind power technology, with turbines growing in size to nearly 7.5 MW. As of 2011, more than 83 countries around the world were using wind power on a commercial basis [1]. Over the last five years, the average annual growth of wind power has been 26.3% per year, and it is expected that 12% of the world's electricity consumption will be provided by wind power by 2020 [2, 3]. In the United States (US), the department of energy estimates that to achieve 20% of the US energy needs from wind by 2030, the number of wind turbine installations will increase from approximately 2000 units per year in 2006 to almost 7000 units per year in 2017 [4]. Thus, increasing the maximum power capture, improving the overall operational range, minimizing the costs, and expanding the use of the wind turbines for both onshore and offshore applications will be steadily among the main goals in the wind power industry.

A wind turbine converts the captured kinetic energy in the wind to electrical energy through a generator. The wind generator technology is improving and the current concepts are continuously advanced. Earlier research has shown that due to varying wind speeds, and consequently the changing rotational speeds of the rotor, variable speed drives result in a higher wind power capture compared to drives operating at one constant speed [5, 6, 7]. Figure 1 shows the power curve of a typical variable speed pitch control wind turbine. There is not any power being supplied if the wind speed is less than a minimum value called the cut-in speed. The optimum wind turbine performance is achieved when the wind speed reaches to the rated speed of the wind turbine (region two), and the power generation will be stopped at the cut-out speed to prevent any possible structural damage [2, 8].

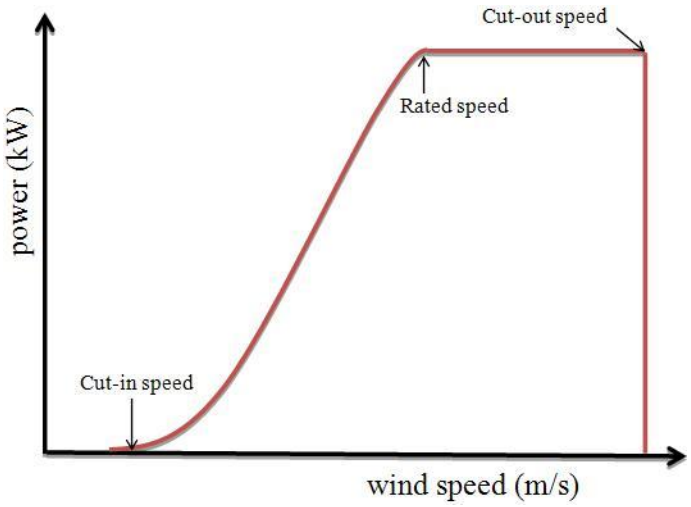

Figure 1 A typical power curve of a wind turbine

Control strategies of variable speed pitch control wind turbines are implemented by the pitch and generator torque controllers. Figure 2 shows the power coefficient (C_P) curves for different pitch angles versus the tip speed ratio (λ) which is the ratio between the rotational speed of the tip of a blade and the actual velocity of the wind [9]. It is seen that increasing the pitch angle will decrease the maximum C_P value [9]. Thus, from low (cut-in) to medium (rated) wind speeds, a fixed pitch angle blade is designed to allow the wind turbine to operate at its optimum condition, and when the rated speed is reached, a variable pitch mechanism decreases the aerodynamic power, which keeps the wind turbine work at its rated power [9]. The generator torque in the low to medium wind speed region is used to obtain the maximum C_P values, and above the rated speed, it is used to smooth the output power [8]. While larger capacity generators will generate more power, they will have higher torque losses, especially at low wind speeds, and need higher initial rotational speeds to start generating useful power [2, 8]. Decreasing the generator electromechanical losses will increase the efficiency of a wind turbine, especially in the low wind speed region.

US patent numbers 7863789 and 6492753 describe a brushless permanent magnet electrical machine with a fixed air gap that is operated to have a much higher speed than the normal speed by eliminating the induced magnetic torque loss in the generator [10, 11]. This concept in a different way can be used in a wind turbine to employ a higher capacity generator in both the low and high wind speed regions to capture more wind power in the entire operational range of the wind turbine.

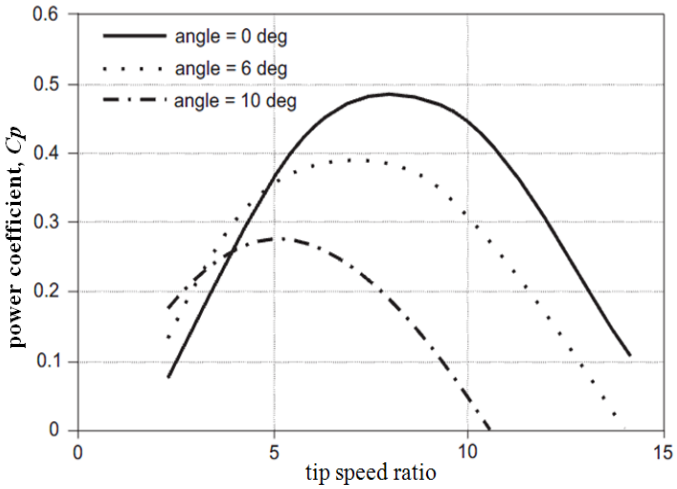

Figure 2 The power coefficient versus the tip speed ratio for different pitch angles

In this work, the possibility of expanding the operational range of an existing wind turbine, mainly by decreasing the cut-in speed, and replacing the current generator with a larger capacity one with better efficiency in the entire operational range of the wind turbine is investigated theoretically by introducing a variable electromotive-force generator (VEG). A combination of aerodynamic and electromagnetic principles together with mathematical methods is used to evaluate the effectiveness of this new feature. A control model of a VEG is proposed. The results on a 1.65 MW wind turbine generator show that it can be modified to start generating power at lower wind speeds than the current cut-in speed of the wind turbine, and it can be replaced by a modified larger capacity generator to produce higher rated power at higher wind speeds and still start generating power at lower wind speeds, by using a VEG.

2. METHODOLOGY

The proposed VEG design is applied to the NM-72 wind turbine with the gross properties shown in Table 1 and the C_P curve shown in Fig. 2 [12]. The NM-72 wind turbine is a conventional three-bladed upwind variable speed, variable blade-pitch-to-feather-controlled wind turbine. The VEG feature is studied under the assumption that the wind turbine has constant blade aerodynamic, structural, hub, nacelle, transmission, and tower properties.

Table 1 Gross properties of the NM-72 wind turbine

Rating	1.65 MW
Rotor orientation, configuration	Upwind, 3 blades
Control	Variable speed, Active stall
Drive train	High speed, multiple-stage gearbox
Rotor diameter	72m
Swept area	4072 m^2
Cut-in, rated, cut-out wind speed	4 m/s, 13 m/s, 25 m/s

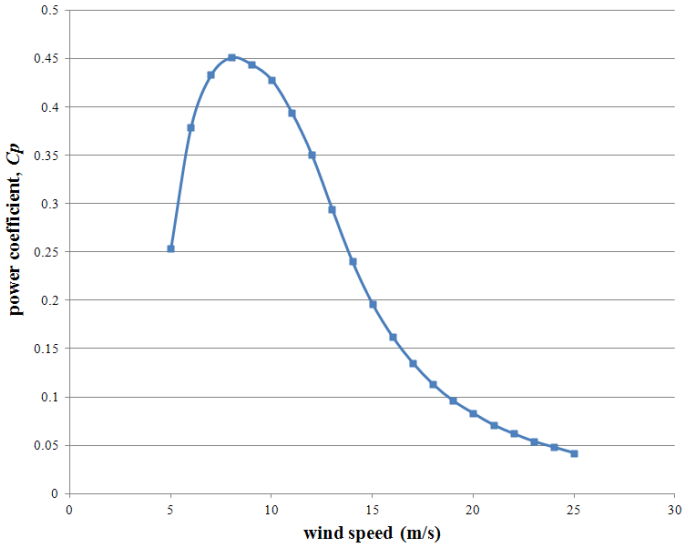

Figure 3 Actual C_P curve of the NM-72 wind turbine for different wind speeds

2.1 Input Wind Power

The output rotor power of a wind turbine is defined as the amount of wind power captured by the rotor of the wind turbine [8]:

$$P_r = \frac{1}{2}\rho A U^3 C_P \eta_{mech} \tag{1}$$

where P_r is the output rotor power, ρ is the air density, A is the rotor swept area, U is the horizontal wind speed that is perpendicular to the turbine plane, C_P is the non-dimensional power coefficient that represents the fraction of the wind power that is extracted by the rotor, and η_{mech} is the mechanical efficiency of the drivetrain.

The rotor swept area is constant and the air density can be calculated as a function of elevation and temperature [13]:

$$\rho = \left(\frac{P_0}{R_g T_e}\right)\exp\left(\frac{-gz}{R_g T_e}\right) \tag{2}$$

where P_o is the standard sea-level atmospheric pressure (101325 Pa), R_g is the specific gas constant (287.04 J/(kg · K) for dry air), T_e is the temperature (287 K at sea-level conditions), Z is the site elevation above the sea level, and g is the gravitational constant (9.8 m/s^2). Substituting the numerical values of P_o, R, and g into Eq. (2) yields

$$\rho = \left(\frac{353.05}{T_e}\right)\exp\left(-0.034\frac{z}{T_e}\right) \tag{3}$$

The air density for the NM-72 wind turbine at $Z = 70$ m, at standard sea level conditions, is $\rho = 1.215$ kg/m^3. The change in the temperature from the sea level to the wind turbine hub, which is approximately 0.05 K, is assumed to be negligible [8].

The linear momentum theory models a turbine as a uniform actuator disk that creates a discontinuity of pressure in the stream tube of air flowing through it [8]. The flow is assumed to be steady state, homogeneous, and incompressible with no frictional drag. It is also assumed that there is a uniform thrust over the disk with an infinite number of blades that has a non-rotating wake. In addition, the static pressure far from upstream and far downstream of the rotor is assumed to be equal to the undisturbed ambient static pressure. With the use of the linear momentum theory analysis the power coefficient of a wind turbine can be defined as [8, 14, 15]:

$$C_P = 4\alpha\left(1-\alpha\right)^2 \tag{4}$$

where α is the induction factor, which is the fractional decrease in the wind velocity between the free stream and the rotor plane. The maximum value for C_P can be found by taking the derivative of Eq. (4) with respect to α and setting it to zero. This will give $C_{Pmax} = 0.5926$ for an ideal wind turbine, which is known as the Betz limit.

For the NM-72 wind turbine with constant properties, the output rotor power can be changed with C_P and the wind speed. At low wind speeds, the only way to keep the output power constant or reduce its decreasing rate with the wind speed is to keep C_P as high as possible. The C_P values at low wind speeds are usually not available in wind turbine data sheets. There are different methods in the literature to estimate the output powers of wind turbines [16-20]. In this work, three methods to estimate the C_P values of the NM-72 wind turbine in the low wind speed region using aerodynamic and mathematical techniques are provided.

2.1.1 The First Method. The first method is the curve fitting method. Figure 4 shows the actual C_P curve of the NM-72 wind turbine versus the wind speed, and its fitted curves with polynomials of different orders under the assumption that $\eta_{mech} = 1$. It illustrates that the fourth-order polynomial gives the best agreement with the actual C_P curve. The estimated C_P values from the fourth-order polynomial curve fit, at wind speeds lower than 8 m/s, are compared with the corresponding actual C_P values in Table 2. Note that the C_P values are assumed to be zero at very low wind speeds where the C_P values are not available or are negative from the curve fit.

Table 2 Comparison of the actual C_P values and the estimated ones from the fourth-order polynomial curve fit

Wind Speed (m/s)	Actual *Cp*	Estimated *Cp*
2	0	0
3	0	0.0352
4	0	0.1578
5	0.253	0.2795
6	0.379	0.3664
7	0.433	0.4227

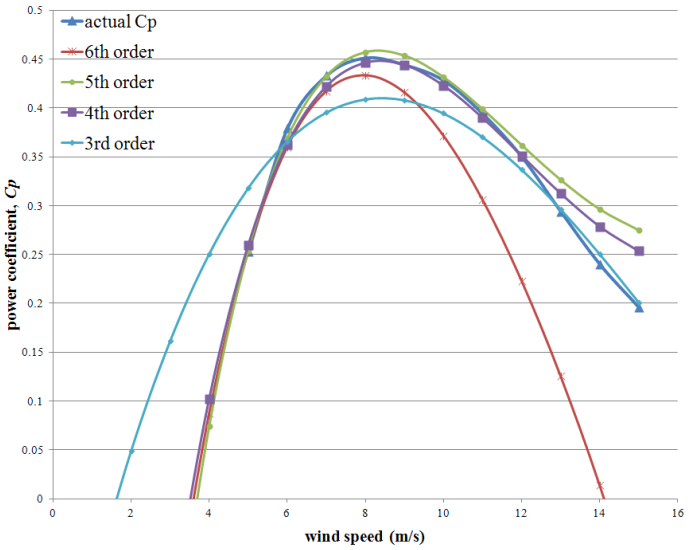

Figure 4 The actual C_P curve of the NM-72 wind turbine and its fitted curves with polynomials of different orders

2.1.2 The Second Method. For a linear wind turbine that has a linear relationship between the change of the rotor power and the wind speed from the cut-in speed to the rated speed, the power coefficient is [16, 21]

$$C_P = 6.75 C_{P\max} \frac{U_{ci}^3}{U^3}\left(\frac{U}{U_{ci}} - 1\right) \tag{5}$$

where U_{ci} is the cut-in speed of a wind turbine. Figure 4 shows the actual power curve (non-linear) of the NM-72 wind turbine, which has a nonlinear relationship between the rotor power and the wind speed, and the estimated linear one. The good agreement of the nonlinear and linear power curves in the low wind speed region suggests the use of Eq. (5) in obtaining the C_P values, which is the second method discussed here.

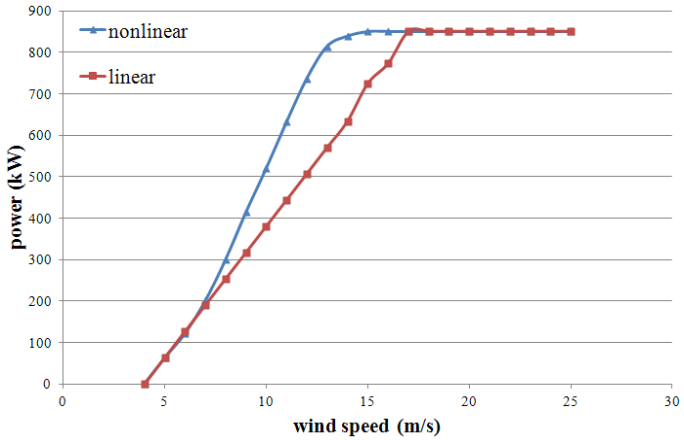

Figure 5 Actual and estimated linear power curves of the MN-72 wind turbine

At the wind speed equal to *5* m/s, below which the C_P values of the NM-72 wind turbine are not available, as shown in Fig. 3, the maximum power coefficient C_{Pmax} in Eq. (5) is assumed to be the C_P value of the NM-72 wind turbine. Calculations under the same assumptions made in the 1-D momentum theory show that, in order to have a monotonically increasing C_P with the wind speed [8], the cut-in speed is estimated to be *2.5* m/s. Figure 6 shows the C_P values of the NM-72 wind turbine in the low wind speed region. The C_P values obtained from the second method at wind speeds lower than *6* m/s are compared with the corresponding actual C_P values in Table 3.

Table 3 Comparison of the actual C_P values and the estimated ones from the second method

Wind Speed (m/s)	Actual *Cp*	Estimated *Cp*
2	0	0
3	0	0.19
4	0	0.24
5	0.253	0.253
6	0.379	0.379

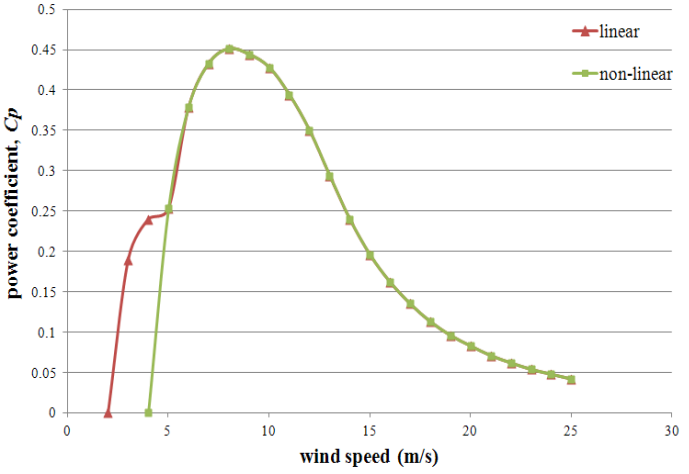

Figure 6 The actual C_P curve of the NM-72 wind turbine and its estimated curve from the second method

2.1.3 The Third Method. The third method is to estimate the highest possible C_P values of the NM-72 wind turbine at wind speeds lower than 8 m/s at which the wind turbine has its C_{Pmax}. The same assumptions made for the 1-D momentum theory, besides the Betz limit and the maximum power coefficient of the NM-72 wind turbine, are considered in obtaining the highest possible C_P values. The mechanical efficiency is not assumed to be one and it can be changed as a result of modifying the generator specifications. Table 4 shows the actual C_P and output rotor power values of the NM-72 wind turbine at wind speeds lower than 8 m/s.

Table 4 Actual C_P and output power values of the NM-72 wind turbine

Wind Speed (m/s)	*Cp*	Power (kW)
2	0	0
3	0	0
4	0	0
5	0.253	78.235
6	0.379	202.519
7	0.433	367.412
8	0.451	571.240

At a high wind speed, the output rotor power is dominated by the wind speed rather than the C_P value. While at wind speeds higher than the rated speed, pitch control is used to reduce the C_P value, more wind power will be captured from low to medium wind speeds by having the maximum C_P values at different wind speeds. At low wind speeds, increasing the C_P values or the mechanical/electrical/magnetic efficiency of the NM-72 wind turbine, without changing such specifications as the hub height and the rotor swept area, are the main options to obtain higher output power values.

Table 5 shows the procedure of the third method to determine the highest C_P values of the NM-72 wind turbine in the low wind speed range. In each column in Table 5, the last row shows the actual C_P value at a particular wind speed. Other rows are the required $C_P\eta$ values at lower wind speeds to get the same output rotor power at these wind speeds. The Betz limit and the maximum power coefficient of the NM-72 wind turbine, which are two possible limits, are considered. For instance, the C_P value at *8 m/s* is *0.45*, which corresponds to an output rotor power of *571* kW. To keep this output rotor power at a lower wind speed such as *7* m/s, the $C_P\eta$ value should be increased to *0.672*, which is higher than the Betz limit. While it is impossible to reach this value at *7 m/s*, a maximum C_P value can be determined to increase the output rotor power. Another case of interest is when the wind speed is at *5* m/s. To generate power at *4* m/s equal to that at 5 m/s, $C_P\eta$ should be *0.493*. It is impossible again to reach this value with the existing configuration of the wind turbine that has C_{Pmax}=0.45. Table 6 and Fig. 7 show the comparison of the actual *Cp* values of the NM-72 wind turbine and the estimated ones from the third method in wind speeds from *1* m/s to *7* m/s.

Table 5 Procedure of the third method to determine the highest C_P values of the NM-72 wind turbine in the low wind speed range

Wind Speed (m/s)	8	7	6	5
1	230.582	148.31	81.747	31.58
2	28.82275	18.53875	10.21838	3.9475
3	8.540074	5.492963	3.027667	1.16963
4	3.602844	2.317344	1.277297	0.493438
5	1.844656	1.18648	0.653976	0.25264
6	1.067509	0.68662	0.378458	
7	0.672251	0.432391		
8	0.450355			

Table 6 Comparison of the actual C_P values and the estimated ones from the third method

Wind Speed (*m/s*)	Actual *Cp*	Estimated *Cp*
1	0	0
2	0	0.1
3	0	0.172
4	0	0.26
5	0.253	0.34
6	0.379	0.41
7	0.433	0.443
8	0.451	0.451

With a good approximation, the C_P values of the NM-72 wind turbine in the low wind speed range from 0.959 m/s to 8 m/s can be found using the following equation:

$$C_P = 0.0009U^3 + 0.0072U^2 + 0.0657U - 0.0688 \qquad (6)$$

which has an error of around at most 1% compared with the actual C_P values for different wind speeds. Figure 8 shows the comparison of the actual power curve of the NM-72 wind turbine and the estimated one using the $C_P\eta$ values from the third method at wind speeds lower than *7* m/s. It shows that there can be a significant decrease in the cut-in speed of the wind turbine with a modified generator with a reduced torque loss. Table 7 is provided with C_P values and output powers of the actual and modified NM-72 using Eq. (6).

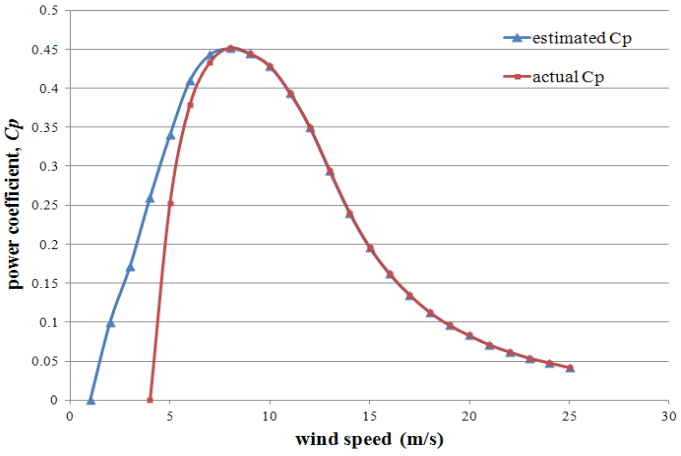

Figure 7 The actual C_P curve of the NM-72 wind turbine and its estimated one from the third method

Table 7 Estimated Cp values and output powers of the NM-72 wind turbine from the new cut-in speed to *8 m/s*

Wind speed (m/s)	Cp	New power (kW)	Actual power (kW)
0.959	0.0000	0.0001	0
2	0.0842	1.6664	0
3	0.1688	11.2748	0
4	0.2516	39.8348	0
5	0.3272	101.1801	78.235
6	0.3902	208.5033	202.519
7	0.4352	369.2793	367.412
8	0.4568	578.5861	571.240

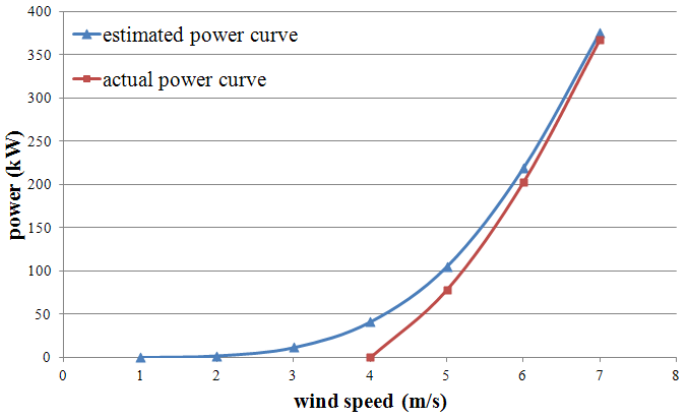

Figure 8 Comparison of the actual and estimated power curves of the NM-72 wind turbine at wind speeds lower than 7 m/s

Having smoother changes in *Cp* values at low wind speeds and expanding the operational range of the wind turbine are remarkable consequences of the third method. While the improved power curve here is obtained by a semi-ideal method, modern wind turbines with more advanced technologies in rotor blade design and higher efficiency drivetrains will eventually have power curves similar to that in Fig. 8.

Any changes in the output rotor power in Eq. (1) due to the changes in the parameters there can be found using the MATLAB/Simulink model shown in Fig. 9, where it is assumed that $\eta_{mech} = 1$. More details on aerodynamic aspects of the wind turbine in calculating the optimum C_P values and increasing the efficiency of the rotor can be found in the literature [22-26].

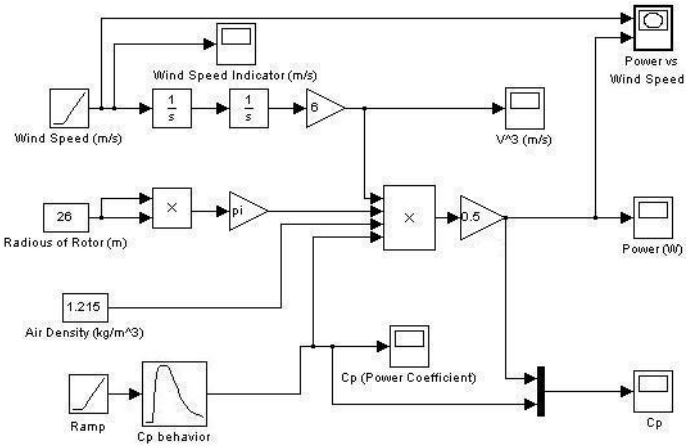

Figure 9 Wind turbine output rotor power MATLAB/Simulink model

2.2 Why Is a VEG Useful for Wind Turbines?

There are regions all around the world that have large differences between the minimum and maximum mean wind speeds throughout a year. For instance, the monthly mean wind speed distribution at the Thasala district in Thailand in 2008 is shown in Table 8 [27]. While the annual mean wind speed in this area was *8.7* m/s in 2008, the monthly mean wind speeds fluctuated between *3* m/s and *15* m/s in different months. There were five months with monthly mean wind speeds lower than *6* m/s; the monthly mean wind speeds in the rest seven months were higher than *8* m/s. A precise technical, environmental, and economical study can be conducted to optimize the wind turbine design to capture the most wind power in this region in different months. However, a significant amount of wind power in the low and high wind speed regions may not have been captured yet. One question can be if we can capture the most wind power in a region like the Thasala district that has large changes in the mean wind speed throughout a year.

Table 8 Monthly mean wind speed distribution at the Thasala district in Thailand in 2008

Mean wind speed range (m/s)	Percentage in the year
0-6	41.67%
6-10	16.67%
10-13	25%
13-20	16.66%

Figure 9 shows the US wind resource map that displays the annual mean wind speed at the *80* m height from the sea level [28]. While more than 26 states (a little more than 50% of the states in the US) have an annual mean wind speed lower than 6.5 m/s, the areas with annual mean wind speeds at around 6.5 m/s and higher at the 80 m height are generally considered to have suitable wind resource for wind developments [28]. Does it mean that those 26 states cannot be considered to have suitable wind resource for wind developments?

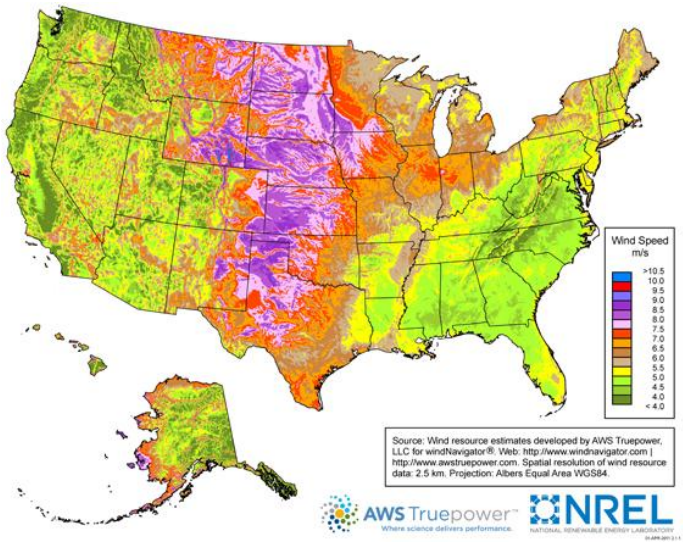

Figure 10 US wind resource map

A key answer to the above two questions is to include a VEG feature in a current wind turbine in a wind farm with a low annual mean wind speed and/or large mean wind speed fluctuations. A larger capacity generator can be employed in a wind turbine to capture more wind power in the high wind speed region and the most wind power in the low wind speed region by the VEG feature. This means moving the rated power line upward in the range of rated speed to cut-out speed of the power curve in Fig. 1, and decreasing the cut-in speed in lower wind speeds, as shown in Sec. 2.1.

2.3 A VEG Concept

The fundamental operation of a synchronous generator or other electrical machines can be understood by applying the induction law on a conductor moving in a static magnetic field [29]:

$$Emf = NB\frac{dA}{dt} = NBI\frac{ds}{dt} = NBl_f v \qquad (7)$$

where Emf is the induced voltage or the electromotive force that is proportional to the time varying flux enhanced by the circuit; l_f and ds are the width and the change in the length of the moving surface area, respectively; and v is the velocity of the moving conductors. In a fixed magnetic field with a constant velocity of the moving conductors, the electromotive force can be changed by changing l_f in the magnetic field.

Figure 11 shows the schematic of a VEG with a movable stator and a fixed rotor. When the wind speed falls in the range between the new cut-in speed of the modified generator, such as that shown in Fig. 7, and the current cut-in speed of a regular generator, the adjustable overlap between the rotor and the stator is implemented to smooth the decreasing rate of the output power of the generator compared with that of the regular generator. The full overlap between the rotor and the stator

occurs when the wind speed is slightly higher than the current cut-in speed and lower than the cut-out speed of the wind turbine to produce the maximum power in this range.

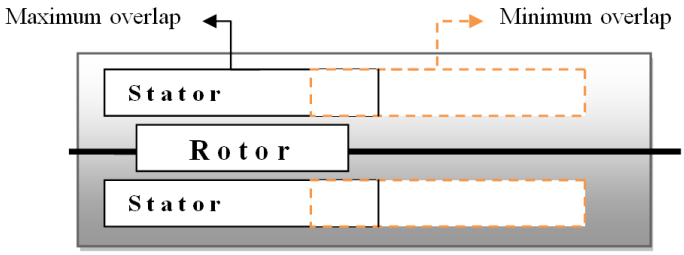

Figure 11 Schematic of a VEG with an adjustable overlap between the rotor and the stator

2.3.1 Mathematical Model. The one-phase equivalent circuit of a synchronous generator of a wind turbine is shown in Fig. 12 [30].

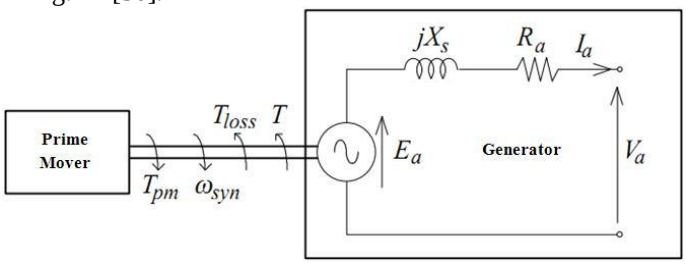

Figure 12 One-phase equivalent circuit of a synchronous generator

At the steady state, the mechanical torque from a prime mover should balance the electromagnetic torque provided by the generator and the torque losses due to friction and wire winding:

$$T_{pm} = T + T_{loss} \tag{8}$$

Multiplying Eq. (8) by the synchronous speed ω_{sys} yields the power balance equation:

$$P_{pm} = P_{em} + P_{loss} \tag{9}$$

where $P_{pm} = T_{pm}\omega_{sys}$ is the mechanical power supplied by the prime mover, $P_{em} = T\omega_{sys}$ is the electromagnetic power of the generator, and $P_{loss} = T_{loss}\omega_{sys}$ includes the mechanical and electrical power losses. Using the phasor analysis, the real power is defined by

$$P_{em} = \frac{E_a V_a}{Z_s}\cos(\theta_s - \delta) - \frac{V_a^2}{Z_s}\cos(\theta_s) \tag{10}$$

where E_a and δ are the magnitude and the phase angle of the induced voltage, respectively, V_a is the terminal voltage, Z_s is the synchronous impedance, and θ_s is the phase angle of the synchronous impedance. If the effective armature resistance is neglected ($R_a = 0$), the magnitude of the synchronous impedance becomes that of the synchronous reactance ($|Z_s| = |X_s|$). The real power and the electromagnetic torque for three phases with $\theta_s = 90^\circ$ can be simplified to

$$P_{em} = \frac{3E_a V_a}{X_s}\sin\delta = P_{\max}\sin\delta \tag{11}$$

$$T_{em} = \frac{P_{em}}{\omega_{syn}} = \frac{3E_a V_a}{\omega_{syn} X_s}\sin\delta \tag{12}$$

Note that Eq. (11) is derived under the assumption of a uniform air gap between the rotor and the stator. In the case of a non-uniform air gap, Eq. (12) becomes [30-32]:

$$T_{em} = \frac{P_{em}}{\omega_{syn}} = \frac{3E_a V_a}{\omega_{syn} X_d}\sin\delta + \frac{3V_a^2}{2\omega_{syn}}\left(\frac{1}{X_q} - \frac{1}{X_d}\right)\sin 2\delta \tag{13}$$

where X_q and X_d are the quadratic-axis and direct-axis synchronous reactances, respectively. With the assumption of a uniform air gap, $X_q = X_d = X_s$. The load angle can be estimated using the phasor diagram [33]:

$$\delta = \arctan\left(\frac{I_a X_S P - I_a R_a Q}{V_a S + I_a X_S Q + I_a R_a P}\right) \tag{14}$$

where Q is the reactance power and S is the apparent power.

2.4 Overlap Adjustment

The rotor power at the current cut-in speed is

$$P_{rci} = \frac{1}{2}\eta_{mech_{ci}} C_{pci}\rho A U_{ci}^3 \tag{15}$$

Where the subscript ci denotes the cut-in speed, U_{ci} is the current cut-in speed, and $\eta_{mech_{ci}}$ and C_{pci} are the mechanical efficiency and the power coefficient at the current cut-in speed, respectively. The ratios of the rotor power and the generated power at any wind speed to those at the current cut-in speed are

$$\frac{P_{ri}}{P_{rci}} = \frac{\eta_{mech_i} C_{pi} U_i^3}{\eta_{mech_{ci}} C_{pci} U_{ci}^3} \tag{16}$$

$$\frac{P_{gi}}{P_{gci}} = \frac{E_{ai}}{E_{aci}} \frac{\sin(\arctan(\frac{I_{ai}X_{Si}P - I_{ai}R_{ai}Q}{V_{ai}S + I_{ai}X_{Si}Q + I_{ai}R_{ai}P}))}{\sin(\arctan(\frac{I_{aci}X_{Sci}P - I_{aci}R_{aci}Q}{V_{aci}S + I_{aci}X_{Sci}Q + I_{aci}R_{aci}P}))} \frac{X_{sci}}{X_{si}} \tag{17}$$

respectively, where the subscript i in P_{ri}, C_{pi}, U_i, P_{gi}, E_{ai}, and δ_i denotes any wind speed. Under the assumptions of $X_S >> R_a$ and the unit power factor of the generator, making use of the power relations and Eq. (7), one has

$$\frac{P_{gi}}{P_{gci}} = \frac{E_{ai}}{E_{aci}} \frac{\sin\delta_i}{\sin\delta_{ci}} \frac{X_{sci}}{X_{si}} = \frac{A_i}{A_{ci}} \frac{\sin(\arctan\left(\frac{X_{Si}}{R_{Li}}\right))}{\sin(\arctan\left(\frac{X_{Sci}}{R_{Lci}}\right))} \frac{X_{sci}}{X_{si}} \tag{18}$$

where A_i and A_{ci} are the areas of the effective moving surfaces at any wind speed and the current cut-in speed, respectively. Thus, the ratio of the overlap between the rotor and the stator at any wind speed to that at the current cut-in speed can be obtained from the corresponding area ratio:

$$\frac{A_i}{A_{ci}} = \frac{P_{ri}}{P_{rci}} \frac{\sin(\arctan\left(\frac{X_{Sci}}{R_{Lci}}\right))}{\sin(\arctan\left(\frac{X_{Si}}{R_{Li}}\right))} \frac{X_{si}}{X_{sci}} \tag{19}$$

For a specific generator, the overlap ratio will be obtained based on the generator specifications and the ratio of the input power at any wind speed to that at the current cut-in speed.

3. RESULTS

The C_P values in the low wind speed region can be estimated using one of the three methods described in Sec. 2.1. To show the overlap adjustment procedure for the NM-72 wind turbine, the third method of estimating the C_P values is used. The fixed output power is assumed to correspond to the wind speed at *7* m/s, at which the ratio of the output rotor powers at wind speeds of 7 m/s and 6 m/s is less than or equal to *1.5*. The input wind power at any wind speed lower than *7* m/s from Eq. (15) should be equal to the output power of the NM-72 wind turbine generator in Eq. (11) under the assumption that there are no mechanical, electrical, and magnetic losses, which means that $\eta = 1$. The ratio of the overlap between the rotor and the stator at any wind speed to that corresponding to the fixed output rotor power can be obtained from the corresponding area ratio:

$$\frac{A_i}{A_{fixed}} = \frac{P_{ri}}{P_{rfixed}} \frac{\sin(\arctan\left(\frac{X_{Sfixed}}{R_{Lfixed}}\right))}{\sin(\arctan\left(\frac{X_{Si}}{R_{Li}}\right))} \frac{X_{si}}{X_{sfixed}} \tag{20}$$

where the subscript $fixed$ in P_{rfixed}, R_{Lfixed}, and X_{Sfixed} denotes the wind speed corresponding to the fixed output rotor power. The reactance and resistance of an existing variable speed synchronous generator at different rotational speeds in [34] are used to obtain the second and third ratio values on the right-hand side of Eq. (20) and their products, as summarized in Table 9. Thus, the area ratio in Eq. (20) can be approximated by

$$\frac{A_i}{A_{fixed}} \approx \frac{P_{ri}}{P_{r_{fixed}}} \tag{21}$$

Table 9 Reactance and load angle ratios and their products at different rotational speeds

Rotational speed (RPM)	Reactance (Ohm)	$\frac{X_{si}}{X_{sfixed}}$	$\frac{\sin(\arctan\left(\frac{X_{Sfixed}}{R_{Lfixed}}\right))}{\sin(\arctan\left(\frac{X_{Si}}{R_{Li}}\right))}$	$\frac{\sin(\arctan\left(\frac{X_{Sfixed}}{R_{Lfixed}}\right))}{\sin(\arctan\left(\frac{X_{Si}}{R_{Li}}\right))} \frac{X_{si}}{X_{sfixed}}$
400	4.1947	1	1	1
350	4.1197	0.9821	0.3862	0.9972
300	4.0447	0.9642	0.3803	0.9945
250	3.9697	0.9464	0.3744	0.9919
200	3.8947	0.9285	0.3685	0.9892
150	3.8197	0.9106	0.3625	0.9867
100	3.7447	0.8927	0.3564	0.9841
50	3.6697	0.8748	0.3503	0.9817
0	3.5947	0.8570	0.3442	0.9792

Table 10 and Fig. 13 show the results of the overlap adjustment procedure at different wind speeds. The change in the overlap is zero at the wind speed corresponding to the fixed output rotor power, and it increases as the wind speed decreases.

Table 10 Percentages of overlap changes at different wind speeds

Wind speed (m/s)	Percentage of changing the overlap
0.959	100.00
2	99.55
3	96.95
4	89.21
5	72.60
6	43.54
7	0

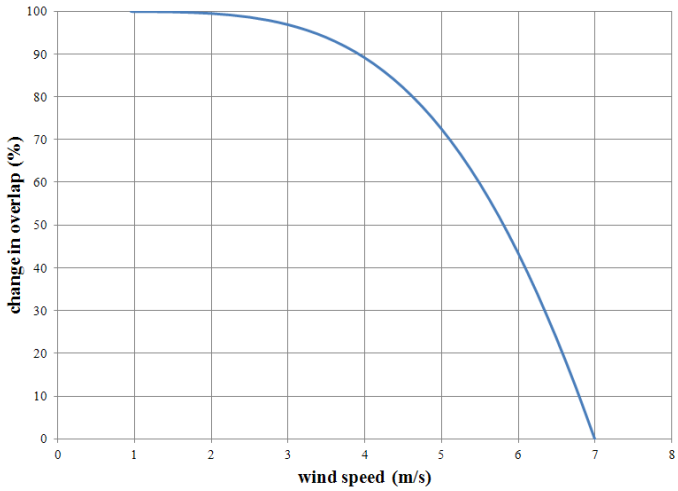

Figure 13 Percentages of overlap changes at different wind speeds

3.1 Application of the VEG in a Wind Farm

The analysis of the wind speed distribution at the Thasala district in Sec. 2.2 is used to show the impact of using the VEG in the NM-72 wind turbine to expand the operational range and capture more wind power at low wind speeds. Wind speeds at different heights can be obtained by the power law [13]:

$$U_2 = U_1 \left[\frac{H_2}{H_1} \right]^{\tau} \tag{22}$$

where V_2 is the unknown wind speed at height H_2, V_1 is the known wind speed at the measurement height H_1, and τ is the wind shear component. The wind shear component is usually assigned a value of 0.143, known as the $1/7^{th}$ power law, to predict the wind profile in a well-mixed atmosphere, over a flat and open terrain. However, higher exponent values are usually observed either in the low to medium wind speed (lower than 7 m/s or 16 mph) range or on vegetated surfaces [13].

The wind shear component can be obtained using available wind speed data at 20 m, 30 m, and 40 m heights and Eq. (22). Table 11 shows the monthly mean wind speeds at the NM-72 wind turbine hub height using the estimated wind shear components and Eq. (22). The minimum and the maximum wind speeds at the NM-72 wind turbine hub height at the Thasala district were *3.817* m/s and *14.745* m/s, respectively. There were five months with monthly mean wind speeds lower than *6* m/s; the monthly mean wind speeds in the rest seven months were higher than *8* m/s with the maximum mean wind speed at around *15* m/s in January.

Table 11 Monthly mean wind speed distribution at the Thasala district

Month	Mean wind speed			
	20 m	30 m	40 m	70 m
January	5.03	6.45	9.12	14.745
February	6.72	7.80	9.36	12.231
March	6.85	8.12	9.23	11.743
April	5.05	7.04	8.19	12.101
May	4.35	6.70	8.02	13.142
June	4.33	6.59	6.84	9.894
July	4.51	6.40	4.82	5.086
August	2.16	3.03	2.96	3.817
September	2.38	3.29	3.37	4.462
October	4.27	5.91	6.08	8.087
November	2.55	4.06	4.10	6.016
December	3.18	4.02	4.27	5.417

For a low mean wind speed region like the Thasala district with high mean wind speeds in certain months, a modified larger capacity wind turbine generator equipped with the VEG feature can be employed to expand the operational range of the wind turbine by decreasing the minimum wind speed required for it to generate useful power and capture more wind power in both high and low wind speed months. Figure 14 shows how a modified 2 MW wind turbine equipped with the VEG feature can capture more wind power in a larger operational range compared with the current 1.65 MW wind turbine.

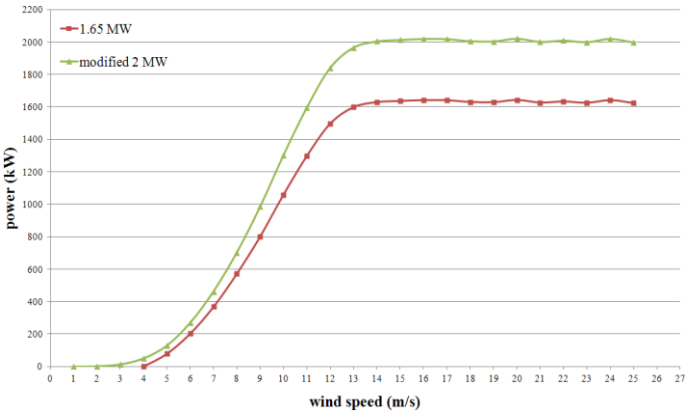

Figure 14 Comparison of the power curves of the current 1.65 MW and the modified 2 MW wind turbine

Figure 15 compares the power curves of the current 1.65 MW wind turbine with those of the modified 1.65 MW and the modified 2 MW wind turbine in the low wind speed region. A modified larger capacity generator can capture more wind power in the entire operational range of the wind turbine, including the low wind speed region with wind speeds lower than the current wind turbine cut-in speed.

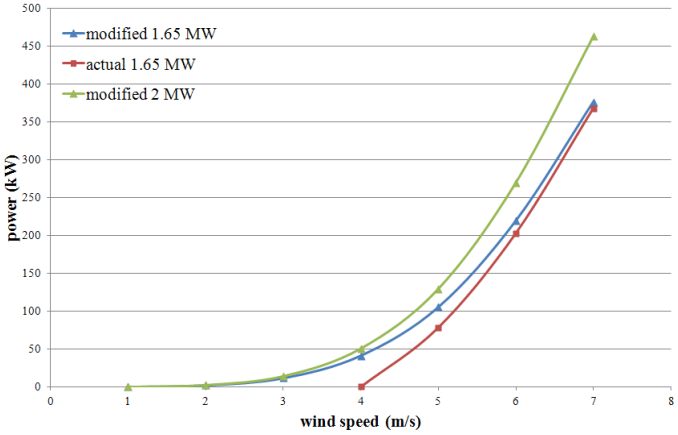

Figure 15 Comparison of the power curve of the current 1.65 MW wind turbine with those of the modified 1.65 MW and the modified 2 MW wind turbine in the low wind speed region

3.2 Economics of the VEG

In order for the VEG feature to have a market impact, its economic implications are addressed here. If the cost involved with using the VEG in place of the market standard generator is significantly high relative to the increased efficiency observed, then such an implementation would not be economically viable. Thus, consideration to the cost of construction, efficiency, and kilowatt-hour pricing is outlined to support the claims of economic feasibility of the VEG feature.

The largest barrier to wind power as a major power source is the high cost of wind turbine construction. Table 12 outlines the cost associated with the construction of a 1.65 MW onshore wind turbine like the NM-72 wind turbine [35]. By breaking the total cost of a wind turbine construction into the price for each component, sensitivity analysis can be applied to price change assumptions about individual components and determine the overall price change of the wind turbine resulting from using the VEG over the market standard generator [36]. The generator of a 1.65 MW onshore wind turbine comprises about 5.5% (around $250,000 based on 2011 US dollars) of the total cost of the wind turbine construction and maintenance. Since this means that the generator comprises 9.5% of the total wind turbine capital cost, changes in the generator pricing can have a relatively significant impact on the construction cost of a wind turbine. Note that this pricing only applies to onshore wind turbines with a 1.65 MW rating; offshore wind turbines will have lower individual component percentages of the total construction and maintenance cost, since the balance of the plant cost is higher. Higher power rated wind turbines will experience economies of scale, resulting in lower cost per megawatt pricing of components. By establishing the basic pricing for a standard generator, an increase in the efficiency between the standard market generator and the VEG is observed.

Table 12 The cost associated with the construction of a 1.65 MW onshore wind turbine

Onshore Wind Turbine	**1.65 MW**
Rotor	
Blades (3)	$384,454.40
Hub	$107,289.60
Pitch mechanism and bearings	$107,289.60
Drive-Train, nacelle	
Low-speed shaft	$53,644.80
Bearing	$31,292.80
Gearbox	$384,454.40
Mechanical brake	$8,940.80
Generator	**$245,872.00**
Power electronics	$299,516.80
Yaw drive and bearings	$49,174.40
Main frame	$232,460.80
Electrical connections	$151,993.60
Hydraulics, cooling system	$44,704.00
Nacelle cover	$53,644.80
Control, safety System, condition monitoring	$89,408.00
Tower	$371,043.20
Wind turbine capital cost	$2,615,184.00
Foundation	$105,664.00
Transportation	$113,792.00
Roads, civil work	$182,880.00
Assembly and installation	$85,344.00
Electrical lines and connection	$280,416.00
Engineering and permits	$73,152.00
Decommissioning, scour project	$81,280.00
Balance of plant cost	$922,528.00
Levelized replacement cost (20 Years) (LRC x 20 Years, CF = 0.3)	$247,904.00
Regular maintenance cost (20 Years) (Operation & maintenance x 20 Years, CF = 0.3)	$329,184.00
Fees (20 Years) (Fees x 20 Years)	$182,880.00
Operating expenses (20 Years)	$759,968.00
Total	**$8,595,360.00**

Table 13 details the output powers of a current 1.65 MW wind turbine and the modified 1.65 MW and 2 MW wind turbines using the wind speed distribution at the Thasala district in Table 11. Efficiency in Table 9 is calculated based on the ratio of the maximum possible output power of a wind turbine to its actual or estimated value throughout a year in the Thasala district. Up to 2% increase in the efficiency can be achieved for the modified 1.65MW wind turbine compared with the current one in the entire operational range. With the assumed 20-year life cycle for the 1.65 MW wind turbines, the present value returns (given a 3% discount rate) roughly 6.7% of the total cost of the market standard generator. Sensitivity analysis of the total output powers yields values ranging from

4-8% of the total cost of the market standard generator, which shows that the VEG is economically feasible. As the rated power of the modified wind turbine generator increases, the efficiency between the market standard generator and the modified one increases. Since the cost of an individual wind turbine component increases at a lower rate than the increase in the rated power (doubling the rated power of a wind turbine does not double the price of each component), a greater revenue potential exists in a modified larger capacity wind turbine to a current one in regions with high probabilities of low wind speeds.

Table 13 Comparison of the output powers of the current 1.65 MW wind turbine and the modified 1.65 and 2 MW wind turbines

Mean wind speed range (m/s)	Percentage in a year (%)	Approximated power generation (MWh)		
		Current 1.65 MW	Modified 1.65 MW	Modified 2MW
0-6	41.67	317	425	526
6-10	16.66	1036	1036	1440
10-13	25	3226	3226	3953
13-20	16.67	2340	2340	2852
Total		6919	7027	8771
Efficiency (%)		47.87	48.62	60.68
Annual Revenue Generating Potential (Levelized Cost of Energy = $0.1018/kWh)		$70,435.42	$71,534.86	$89,288.78

3.3 Control Model

Figure 16 shows a feedback control model of the overlap adjustment procedure at different wind speeds. The output rotor powers at different wind speeds are obtained from Eq. (1); that corresponding to the current cut-in speed in Eq. (15) is kept as the fixed maximum value. To make the generator keep working at lower wind speeds than the current cut-in speed, the overlap between the rotor and the stator is adjusted so that the induced magnetic torque loss is decreased. A feedback controller can be designed to continuously change the overlap between the rotor and the stator until the relative difference of the generator output power and the output rotor power is less than or equal with a pre-defined value ε. Note that in real applications and under the steady state conditions, mechanical/electrical torque losses of a wind turbine should also be included in the torque loss term on the right-hand side of Eq. (8). The calculation of the overlap ratio is shown in Fig. 16(b); the generator output values can be calculated, as shown in Fig. 16(c). A stepper motor can be used to change the overlap between the rotor and the stator. Figure 17 shows the feed forward control results for the NM-72 wind turbine using the C_P values obtained from the third method in Sec. 2.1. It is assumed that a stepper motor has 200 step changes from a full to a zero overlap between the rotor and the stator. The change in the number of steps is zero at *7* m/s, and it increases as the wind speed decreases. The *100%* change in the overlap occurs at the new cut-in speed around *2* m/s, below which the generator cannot generate any useful power.

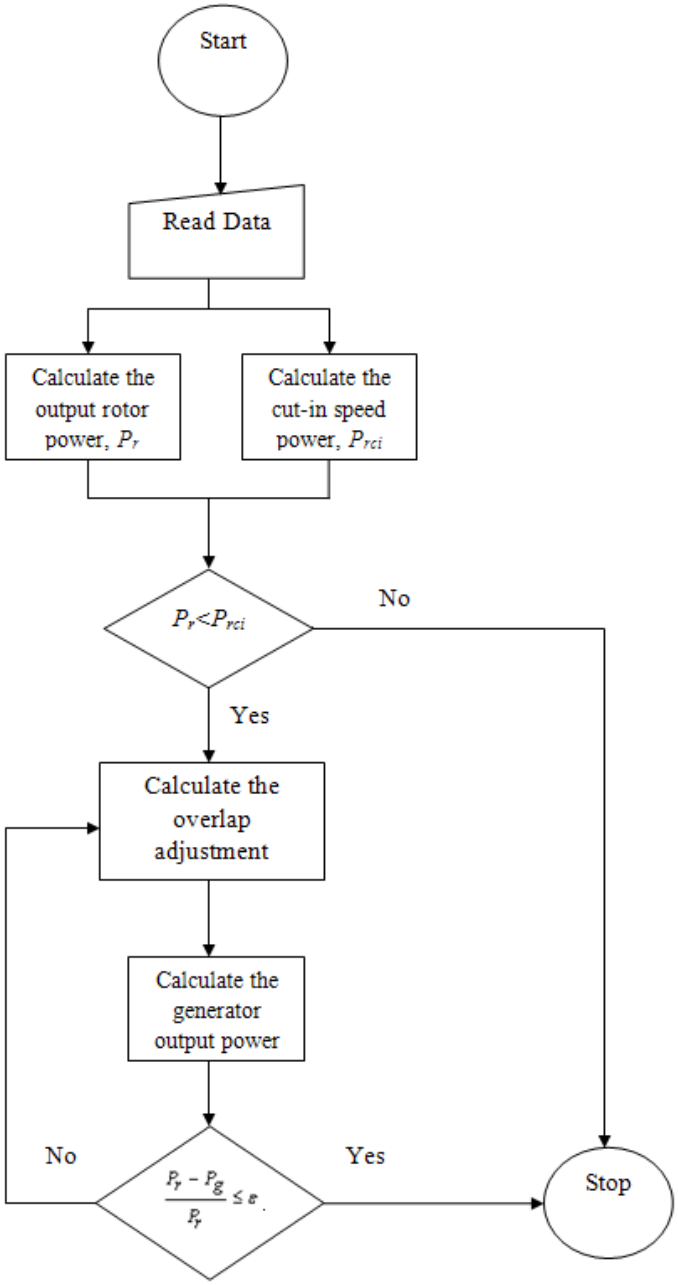

(a)

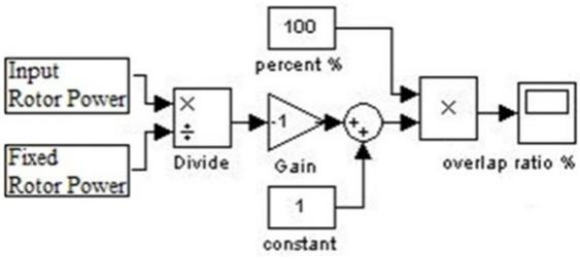

(b)

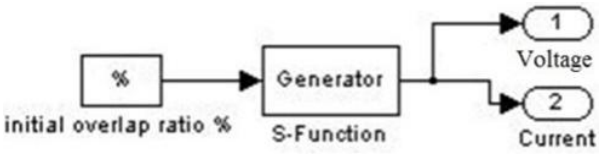

(c)

Figure 16 (a) Flowchart of the overlap adjustment procedure, (b) the overlap ratio calculation, and (c) the generator output power

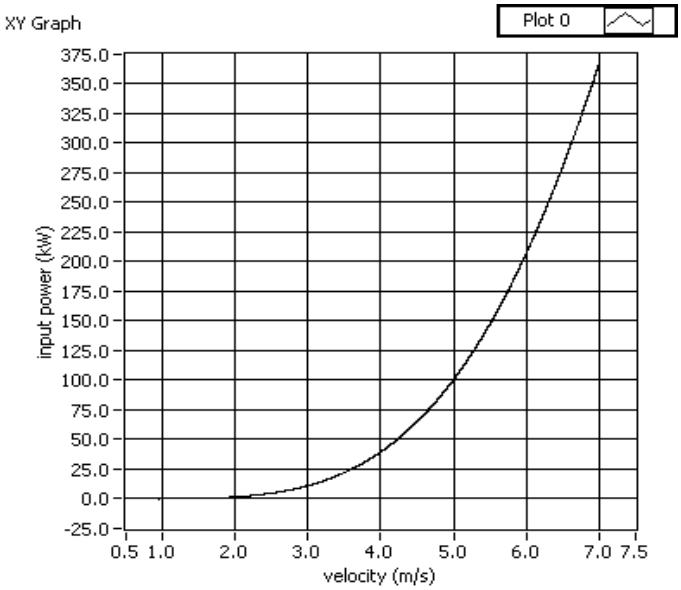

(a)

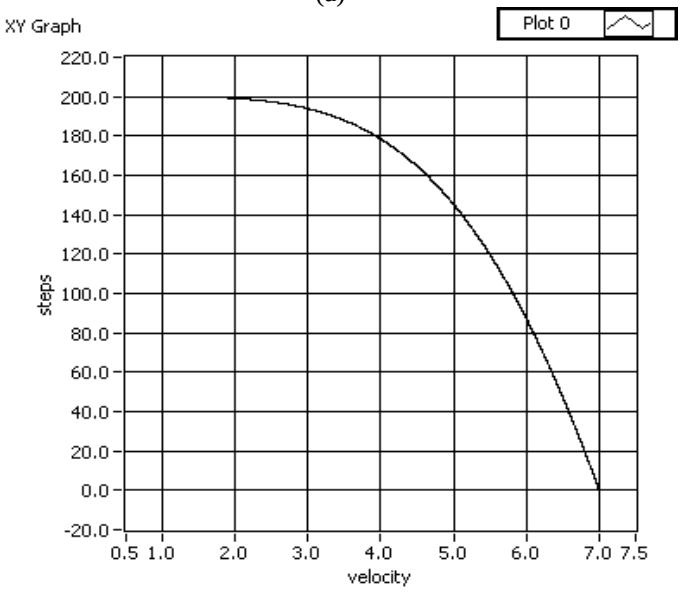

(b)

Figure 17 Results from the overlap adjustment procedure: (a) the input power versus the wind speed, and (b) the change in the steps versus the wind speed

4. CONCLUSION

The development of a VEG for use in wind turbines is theoretically studied using aerodynamic and electromagnetic principles. To calculate the output rotor power of a wind turbine at low wind speeds, three methods for estimating the C_P values are presented. By deriving the mathematical expression of the area ratio, the required overlap adjustment between the rotor and the stator of a VEG is obtained. To implement the overlap adjustment procedure, the generator parameters such as the resistance and the reactance should be accurately determined at different rotational speeds.

The theoretical results of implementing a VEG in a wind turbine indicate significant potentials in expanding the operational range of the wind turbine, capturing more wind power in wind farms with either a low annual mean wind speed or a large difference between the minimum and maximum mean wind speeds, and facilitating achieving higher *Cp* values in the low wind speed range.

5. ACKNOWLEDGMENT

The authors would like to thank the support from the Maryland Industrial Partnership program.

6. REFERENCES

[1] REN 21, 2011, "*Renewable 2011, Global Status Report*," Renewable energy policy network for the 21st century.

[2] Goudarzi, N., 2011,"*Aerodynamic & Electromagnetic Modeling & Analysis of a Variable Torque Generator for Wind Turbine Applications*," Master Thesis, Department of Mechanical Engineering, University of Maryland Baltimore County.

[3] World Wind Energy Association (WWEA), 2011, "*World Wind Energy Report 2010*".

[4] U.S. Department of Energy (DOE), 2008, "*20% Wind Energy by 2030, Increasing Wind's Contribution to U.S. Electric Supply*".

[5] Musgrove, P., 2010, "*Wind Power*," Cambridge University Press, Cambridge, UK, Chap 5.

[6] Chen, Z., and Blaabjerg, F., 2004, "*Wind Turbines-A Cost Effective Power Source*," Przeglad Elektrotechniczny R. 80 NR 5/2004, pp 464-469.

[7] Harrison, R., Hau, H., and Snel, H., 2000, "*Large wind turbines Design and Economics*," John Wiley & Sons Ltd, ISBN 0471-494569.

[8] Manwell, J.F., McGowan, J.G., and Rogers, A.L., 2009, "*Wind Energy Explained; Theory, Design, and Application*," 2nd edition, John Wiley & Sons, Inc., UK.

[9] Muljadi, E., and Butterfield, C. P., 2000, "*Pitch-controlled variable-speed wind turbine generation*," National Renewable Energy Laboratory, Conference Report.

[10] Zepp, L.P., 2011, "*Brushless permanent magnet motor/generator with axial rotor decoupling to eliminate magnet induced torque losses*," US 7863789 B2.

[11] Zepp, L.P., 2002, "*Brushless permanent magnet motor with variable axial rotor/stator alignment to increase speed capability*," US 6492753 B2.
[12] NM72 IEC main specification.
[13] AWS Scientific Inc., 1997," *Wind Resource Assessment Handbook*," National Renewable Energy Laboratory, Chap 9.
[14] Hau, E., 2006, "*Wind Turbines: Fundamentals, Technologies, Application, Economics*," 2nd edition, Springer, Netherlands.
[15] Wilson, R.E., Lissaman, P.B.S., and Walker, S.N., 1976, "*Aerodynamic Performance of Wind Turbines*," E.R.D.A. / NSF/0414-76/1.
[16] Khalfallah, M.G., and Koliub, A. M., 2007, "*Suggestions for improving wind turbines power curves*," the 9th Arab International Conference on Solar Energy (AICSE-9), Kingdom of Bahrain.
[17] Hawkins, T., White, W.N., Hu, G., and Sahneh, F.D., 2010, "*Wind Turbine Power Capture Control with Robust Estimation*," Proceedings of the ASME 2010 Dynamic Systems and Control Conference, Cambridge, Massachusetts, USA.
[18] Dodson, L., Busawon, K., and Jovanovic, M., 2005, "*Estimation of the Power Coefficient in a Wind Conversion System*," Proceeding of the 4th IEEE Conference on Decision and Control, Seville, Spain.
[19] Odgaard, P.F., Damgaard, C., and Nielsen, R., 2008, "*On-Line Estimation of Wind Turbine Power Coefficient using Unknown Input Observers*," Proceedings of the 17th World Congress, Seoul, Korea.
[20] Barnes, D.L., 2005, "*Forecasting an Energy Output of a Wind Farm*," US 7863789 B2.
[21] Martens, A.H.J.A., and Albers, P.H.W.M., 2003, "*Wind Turbine Study, Investigation into CVT Application in Wind Turbines*," Eindhoven University of Technology, Report Number: DCT 2003.90.
[22] Dwinnell, J. H., 1949, "*Principles of Aerodynamics*", McGraw- Hill, New York.
[23] Anderson J.D., 2001, "*Fundamentals of Aerodynamics*", 3rd edition, McGraw Hill.
[24] Verdonschot, M.J., 2009, "*Modeling and Control of wind turbines using a Continuously Variable Transmission*", Eindhoven University of Technology, Report Number: DCT 2009. 280.
[25] Mathew, S., 2006, "*Wind Energy; Fundamentals, Resource Analysis and Economics*", Springer, Netherlands.
[26] Cetin, N.S., Yurdusev, M.A., and Ata, R., Ozdemir A., 2005, "*Assesment of Optimum Tip Speed Ratio of Wind Turbines*", Mathematical and Computational Applications, Vol. 10, No.1, pp. 147-154.
[27] Waewsak, J., Chancham, C., Landry, M., and Gagnon, Y., 2011, "*An Analysis of Wind Speed istribution at Thasala, Nakhon Si Thammarat, Thailand*", Journal of Sustainable Energy and Environment, 2(2), pp.51-55.
[28] AWS Truepower, 2012, "*United States- Annual Average Wind Speed at 80 m*," National Renewable Energy Laboratory.
[29] Wentworth, S. M., 2005, "*Fundamentals of electromagnetic with engineering applications*," John Wiley & Sons, Inc., UK.
[30] Nasar, S.A., and Boldea, I., 1990 , "*Electric Machines, steady-state operation*," Hemisphere Publishing Corp.
[31] Boldea, I., 2006, "*Synchronous Generators*," Taylor and Francis Group. London, UK.
[32] Concordia, C., 1951, "*Synchronous machines, theory and performance*," General Electric Company.
[33] Idzotic, T., Erceg, G., and Sumina, D., 2004, "*Synchronous Generator Load Angle Measurement and Estimation*," ATKAAF, 45(3-4), pp. 179-186.
[34] Edds, M. G., 1980, "*Optimizing Output Power of a Variable Speed Synchronous Generator by Controlling Excitation and Load Resistance*," Master Thesis, University of Massachusetts.
[35] Garcia-Sanz, M., and Houpis, C.H., 2012, "*Wind Energy Systems: Control Engineering Design*," Taylor and Francis Group. London, UK.
[36] George, K., and Schweizer, T., 2008, "*Primer: the DOE Wind Energy Program's Approach to Calculating Cost of Energy*," National Renewable Lab., Report number:SR-500-37653

